Blue lasers on high pressure grown GaN single crystal substrates

S. Porowski, I. Grzegory, S. Krukowski, M. Leszczynski, P. Perlin, and T. Suski
High Pressure Research Center, Warsaw, Sokolowska, Poland

Development of blue and near UV semiconductor light sources has attracted the attention of researchers for several decades. In the sixties, GaN (gallium nitride) and its cousins AlN and InN were already known to be ideal candidates for blue and UV semiconductor light-emitting diodes (LEDs) and laser diodes (LDs). The competitors were zinc selenide based alloys. In the seventies and eighties, the development of ZnSe based LEDs and LDs put that compound much ahead of GaN. In the seventies the development of nitride physics and GaN devices was almost stopped because of two main barriers: the first that the p-type doping method was unknown; and the second that suitable substrates were lacking that would allow the growth of low dislocation-density quantum structures by metal organic vapor-phase epitaxy (MOVPE) and molecular beam epitaxy (MBE).

These barriers were overcome in the early nineties, when Amano, Akasaki [1] and Nakamura [2] discovered p-type GaN doping by Mg and developed the low-temperature buffer layer that lowered the concentration of dislocations in nitride epitaxial layers from 10^{12} to 10^{8} cm^{-2}. The development of the high nitrogen pressure solution growth (HNPSG) method [3] was the important step, which allowed growth of the first dislocation-free GaN epitaxial layers and quantum structures both by MOVPE [4] and MBE [4]. That made it possible to determine many basic physical properties of GaN [5]. These material science achievements and the fact that, in contrast to short lived ZnSe based devices, the nitride based structures remain stable during long laser operation, resolved the ZnSe vs GaN competition. Successful commercialization of blue diodes by Nichia Ltd. and construction of the first blue laser diode by Nakamura in 1996 [6] made GaN based technology the unique solution for blue and UV semiconductor laser diodes of the future.

Despite some progress in reduction of the dislocation density by ELOG (epitaxial lateral overgrowth) technology, the mainstream development effort based on sapphire was slowed down in the late nineties by the lack of progress in reducing the dislocation density below 10^{7} cm^{-2}. The new possibilities were opened by the liftoff technology [7] in which the GaN layer is separated from the sapphire substrate and then is used as a freestanding GaN substrate. This technology is sophisticated and expensive, however it gives GaN substrates with dislocation density about 10^{6} cm^{-2} and reduces thermal stresses in devices. Such two-inch substrates are already available and they serve for construction of blue lasers of a power of hundreds of miliwatts.

We have chosen the alternative way to construct high power lasers. We use lattice matched GaN substrates of low dislocation density, grown by the HNPSG method. The method provides relatively small substrates, about 1 cm^2 in size but, as will be shown, ultra low dislocation density (below 10^{2} cm^{-2}) allows for easier growth of dislocation-free atomically flat quantum structures, which are crucial for the development of high power UV and blue lasers.

Why dislocations are detrimental to high power semiconductor lasers

Dislocations can cause deterioration in the operation of quantum-well based optoelectronic devices mainly by three mechanisms:

a) by serving as nonradiative recombination centers for electrons and holes leading to heat generation instead of optical emission
b) by introducing fast diffusion along the dislocation lines, smearing out quantum wells and p-n junctions
c) by disturbing the epitaxial growth, so that atomically flat structures cannot be obtained.

It turned out that GaN based devices are much more tolerant of the presence of dislocations than classical devices based on GaAs. In these new devices, efficient photo- and electro-luminescence was observed even in materials having dislocation densities as high as 10^{8} – 10^{9} cm^{-2}. For GaAs devices nonradiative recombination related to such high densities of dislocations would quench luminescence almost totally. The effective electro-luminescence was observed for GaN devices with quantum wells containing In ($In_xGa_{1-x}N$ with x between few to 30at% of indium). Nakamura explained this effect as the result of potential fluctuations caused by In segregation, which limits the diffusion length of holes and diminishes dislocation-related nonradiative recombination [8]. From the Nakamura model one can draw two conclusions: i) the presence of dislocations can be detrimental to the efficiency of devices working on a very high level of excitation of carriers such

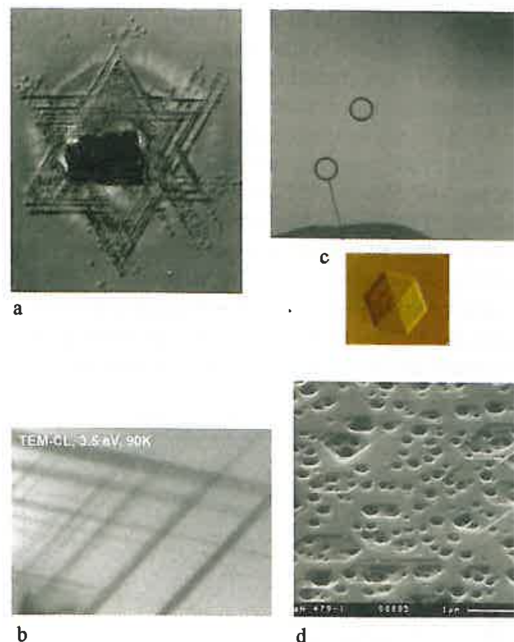

▲ Fig. 1: Dislocations in GaN crystals and layers: a) plastic indentation of high pressure grown GaN single crystal by a diamond pyramid – the dislocations revealed by selective etching surround the hole left by the pyramid [9];
b) cathodoluminescence of this GaN crystal - the black band proving that dislocation related nonradiative recombination quenches the optical emission; c) selective etching of GaN layer grown on a high pressure GaN single crystal; d) selective etching of GaN layer grown on a GaN template deposited on sapphire.

Article available at http://www.europhysicsnews.org or http://dx.doi.org/10.1051/epn:2004301

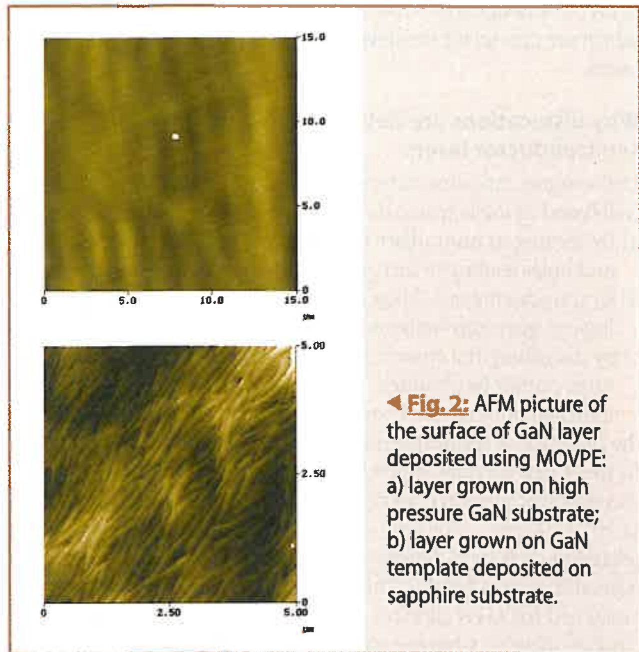

◀ Fig. 2: AFM picture of the surface of GaN layer deposited using MOVPE: a) layer grown on high pressure GaN substrate; b) layer grown on GaN template deposited on sapphire substrate.

as high power laser diodes when the kinetic energy of carriers exceeds the potential barriers created by In segregation; ii) nonradiative recombination due to the presence of dislocations may be especially harmful for devices without indium (for example UV devices based on GaN/GaAlN quantum wells). This was the reason why we have concentrated our efforts towards construction of high power blue lasers and UV devices.

As evidence that the dislocations quench almost totally the luminescence in GaN not containing indium, we show the cathodo-luminescence measurements. In Fig 1a we present GaN grown on high-pressure grown substrates where dislocations were induced by plastic deformation using indentation. In Fig 1b, the dark visible lines are caused by nonradiative recombination on dislocations introduced by plastic deformation. [9].

The effects related to mechanisms (b - diffusion along dislocations) and (c - disturbing epitaxial growth) are also important for the reliability of devices. For instance, in both MOVPE and MBE technologies, the most important growth mode is the step flow. Fig. 2 compares the surface morphology of GaN layers deposited on high-pressure GaN substrates and on a GaN/sapphire template,

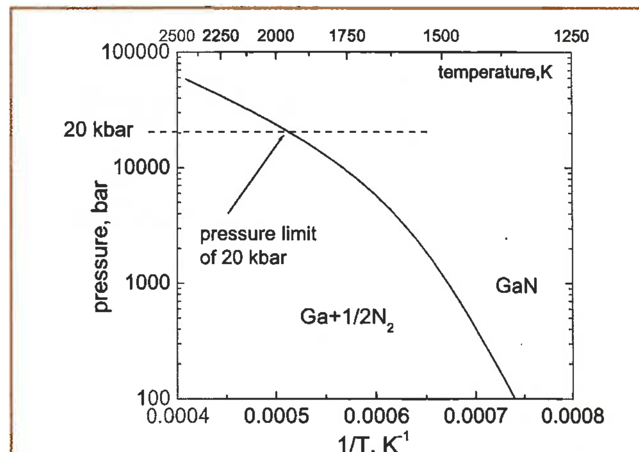

▲ Fig. 3: p-T equilibrium curve for the GaN ⟶ Ga(l) +(1/2) N_2(g) reaction [14].

obtained in the same growth process. As is seen, low dislocation density material has regular straight and parallel atomic steps (Fig. 2a) while material on the template with a five order of magnitude higher dislocation density shows irregular steps with visible dislocations at the ends of the steps (Fig. 2b). Regular step-flow is a prerequisite for obtaining atomically flat quantum wells.

As mentioned above, the dislocations in high power LDs should be avoided. Dimensions of the active part of a typical device are 5-20 μ x 500 μ, which correspond to the area 2.5-10 x 10^{-5} cm^2. Thus the dislocation density below 10^4 cm^{-2} is mandatory for manufacturing the dislocation-free devices. As will be demonstrated in the next Section, high-pressure grown GaN crystals have a dislocation density much below this limit and create possibilities to growth epitaxial structures for such devices..

Substrates – thermodynamics and crystal growth

The GaN binding energy, equal to 9.12 eV/atom-pair, is quite high. For comparison GaAs has a binding energy equal to 6.5 eV/atom-pair. Therefore, as shown in Table 1, the GaN melting temperature is much higher than these for typical semiconductors used in electronics, such as Si, GaP or GaAs.

▼ Table 1: Melting conditions of some elemental and III-V semiconductors

crystal	T^M, K	p^M, bar.
Si	1685	< 1
GaAs	1510	15
GaP	1750	30
GaN – [10]	**2493**	**~ 60 000**

Even more important is the fact that the binding energy of a N_2 molecule is extremely high, equal to 9.72 eV/molecule, which is the highest binding energy of all diatomic molecules [11]. In addition, the enthalpy of evaporation of liquid gallium is relatively high, equal to 2.81 eV/atom [11]. Despite high bonding energy of GaN, the balance of the GaN synthesis reaction: Ga(l) + (1/2)N_2(g) ⟶ GaN(s) is strongly shifted towards the constituents: liquid Ga and gaseous N_2. This fact has extremely important

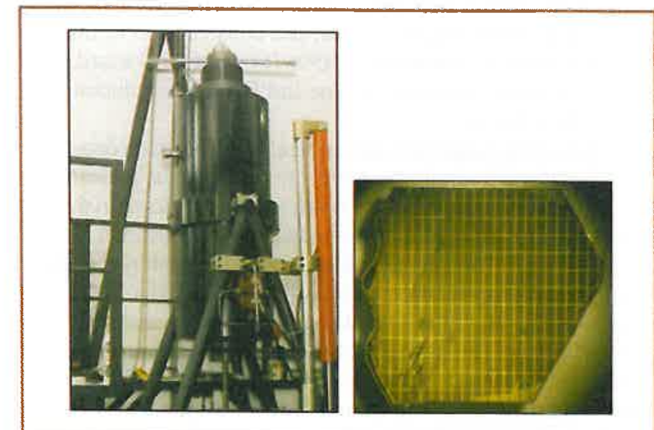

▲ Fig. 4: a) The high-pressure apparatus, constructed in HPRC for crystallization of GaN. The maximum working pressure is 15 kbar, the maximum temperature – 1600°C, the internal diameter – 100 mm; b) GaN crystals grown from solution at high N_2 pressure. The grid size is 1 mm.

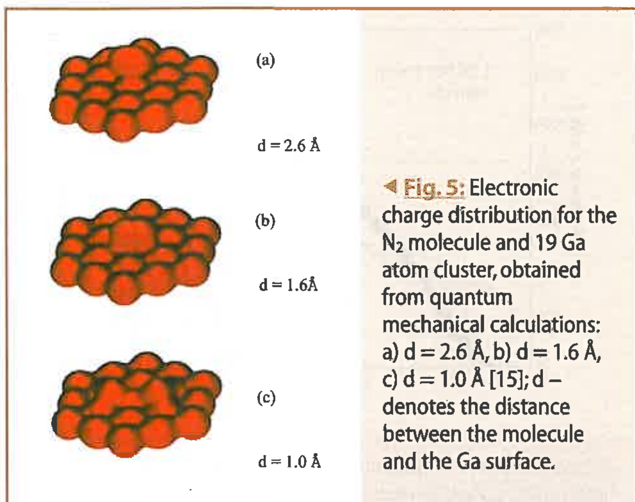

◀ Fig. 5: Electronic charge distribution for the N_2 molecule and 19 Ga atom cluster, obtained from quantum mechanical calculations: a) d = 2.6 Å, b) d = 1.6 Å, c) d = 1.0 Å [15]; d – denotes the distance between the molecule and the Ga surface.

consequences for GaN crystallization because GaN becomes unstable at high temperatures at the normal pressure of nitrogen. As shown in Table 1, the equilibrium nitrogen pressure for GaN at its melting temperature is close to 60 kbar [10]. That pressure is inaccessible for large-volume high-pressure apparatus, thereby rendering impossible the growth of GaN from stoichiometric melt as used in standard Czochralski [12] or Bridgman [13] methods. It has to be crystallized by methods allowing lower temperatures and pressures, from which the solution growth seems to be the best choice.

The method known as high-nitrogen-pressure-solution-growth (HNPSG) is a practical realisation of the GaN synthesis reaction [4]. The HNPSG method relies on a high pressure of nitrogen, which allows an increase in the growth temperature of GaN. The pressure-temperature diagram of GaN stability is shown in Figure 3 [14].

At present, GaN single crystals are obtained in high-pressure gas vessels, that allow working nitrogen pressures up to 20 kbar. These vessels have internal diameters up to 10 cm and volumes up to 4500 cm^3. The crystal growth system is equipped with an internal furnace with graphite multi-zone heaters that allow the temperature to be changed in the two-inch crucible. A view of the high-pressure apparatus is presented in Figure 4a [4].

Growth of GaN proceeds via three consecutive stages: dissolution of nitrogen in liquid gallium, transport of nitrogen in the liquid by convection and diffusion and crystallization in the cold zone. The mechanism of the dissolution of the nitrogen in the liquid gallium was investigated using quantum mechanical calculations [15]. As shown in Figure 5 the nitrogen molecule undergoes dissociation at the gallium surface and then single nitrogen atoms are dissolved in gallium. The calculated energy barrier for N_2 dissociation is 3.4 eV. The barrier is much smaller than the N_2 binding energy (9.72 eV/molecule), indicating that the liquid Ga surface exerts a strong catalytic influence that speeds up the N_2 dissociation and dissolution. After dissolution, the atomic nitrogen is transported to the cold end where the GaN crystal grows from nitrogen rich gallium. The growth of large size good quality GaN crystals requires precise pressure and temperature control during the process.

Due to hexagonal symmetry of its crystallographic wurtzite structure, GaN crystals grown by the HNPSG method usually have the form of hexagonal platelets. The large hexagonal surfaces of bulk GaN crystals correspond to {0001} polar crystallographic planes. Conventionally the Ga-side denoted as the {0001} surface is the one that is used for epitaxy. The side faces of the crystals are mainly the polar {10-11} and also non-polar {10-10} planes [4]. The crystals in the form of hexagonal platelets grow slowly, with a rate below 0.1mm/h into {10$\underline{1}$0} directions (perpendicular to the c-axis). The growth is strongly anisotropic being much slower (about 100 times) in directions parallel to the c-axis. Typical duration of the growth processes is 120 - 200 hours, which gives a crystal with linear size up to 20 mm. These crystals have usually perfect morphology suggesting stable layer-by layer growth. One of these crystals is shown in Fig. 4b.

The high quality of these crystals has been proven by several methods including x-ray diffraction, transmission electron microscopy (TEM), atomic force microscopy (AFM) and selective etching. The typical picture of selective etching of both GaN layers on GaN single crystals and on sapphire is shown in Fig. 1c and d, respectively. Typical high quality high-pressure grown GaN single crystals have a dislocation density not higher than 10^2 cm^{-2} while the best quality GaN layers on sapphire have above 10^7 cm^{-2} [4].

Epitaxy

The structure of GaN homoepitaxial layers follows the structure of the GaN substrates provided that the surface preparation technique and the conditions of the epitaxial growth are properly chosen [17]. As shown before in Fig 2, the atomic step flow on the surface of the homoepitaxial layer is not perturbed and new dislocations are not created. However if we continue to grow layers of AlGaN and InGaN, as necessary to obtain a blue laser structure, the lattice mismatch between GaN and those ternary layers can

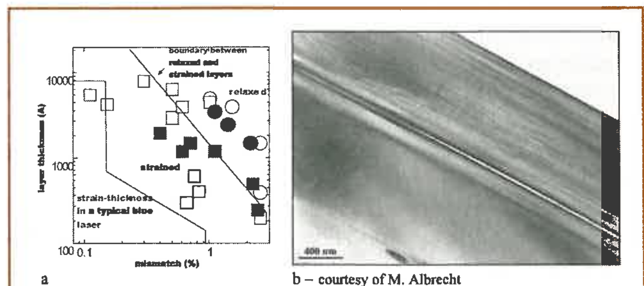

a

b – courtesy of M. Albrecht

▲ Fig. 6: Critical conditions for lattice relaxation for III-N ternaries: a) X-ray data: open circles - AlGaN relaxed, open squares - AlGaN strained, filled squares – InGaN strained, open squares – InGaN relaxed, b) TEM image of the multilayer structure deposited on GaN substrate by MOCVD, the sequence of layers from the lower left corner: n-GaN, n-$Al_{0.11}Ga_{0.89}N$/n-GaN superlattice, n-GaN, $In_{0.09}Ga_{0.91}N$, p-GaN, p-$Al_{0.14}Ga_{0.86}N$/p-GaN superlattice, p – GaN.

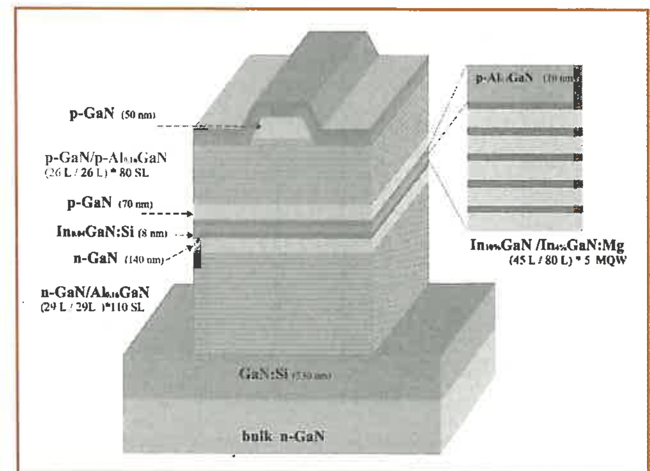

▲ Fig. 7: Structure of GaN laser.

induce misfit dislocations. This phenomenon was analyzed by Domagała et al. [18] by x-ray measurements of lattice parameters for various GaN-based epitaxial layers deposited on GaN substrates as a function of InGaN (AlGaN) composition and thickness. It is shown in Fig 6a that for mismatch and thickness present in a typical blue laser structure, the relaxation of the strain by the generation of dislocations was not observed. In Fig 6b a TEM crossection of the multilayer structure, grown by MOVPE on high-pressure GaN substrate, similar to the blue laser structures is presented. It does not contain dislocations, confirming the results of x-ray measurements.

For laser application we grow GaN/AlGaN/InGaN laser structures in a home-made vertical flow MOVPE reactor and VG Semicon MBE machine. We grow our structure as a separate confinement heterostructure laser, with AlGaN cladding layers and Mg and Si doped GaN waveguides. The active layer of the device is a 5x $In_xGa_{1-x}N/In_{0.024}Ga_{0.976}N$ (QW 0.08<x<0.12) structure consisting of 80Å-thick Si doped barriers and 40Å-thick undoped well layers. The details of the structure are given in the following and are illustrated on Fig. 7.

Contacts and processing – laser device

The devices were processed as ridge-waveguide, oxide-isolated lasers. The mesa structure was etched out in the wafer, down to a depth of 0.3 µm (roughly to the middle of the upper cladding layer). The laser structure was then isolated by e-beam deposition of a 0.2 µm layer of SiO_x. The stripe width is 5-20 µm and the resonator length is 500 µm. The reflectivity of the cleaved mirrors was increased to 50% by coating them with two pairs of quarter-wavelength layers of SiO_2/ZrO_2. The Ni/Au ohmic contacts, of a typical contact resistance $1 \cdot 10^{-4}\ \Omega \cdot cm^2$, were deposited on the top surface of the device, while Ti/Au contacts were deposited on the backside of the highly conducting n-GaN crystal.

The emission wavelengths of the lasers, as presented in Fig. 8, are between 390 and 430 nm. The threshold currents for these lasers are between 380 to 800 mA (for a 15 µm stripe width), while the threshold voltage ranges from 7.5 to 9 V. These values correspond to current densities of 5-10 kA/cm^2. This current density is still a factor of two higher than for the devices manufactured by Nichia and Sony. We attribute this fact to excessive carrier overflow. The slope efficiency of our devices is in the range of 0.25-0.3 W/A per facet (0.5-0.6 W/A for total emission) for the current range 0-3 A. For higher currents the efficiency slightly decreases. Figure 9 shows the basic electrical and optical characteristics of our lasers, all

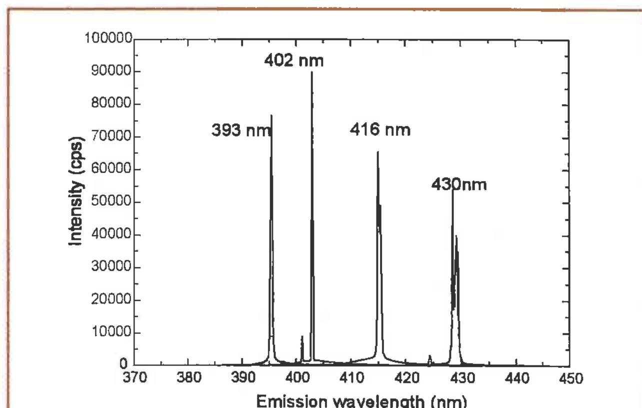

▲ Fig. 8: Emission spectra for laser diodes grown on bulk GaN. Pulse operation is at room temperature.

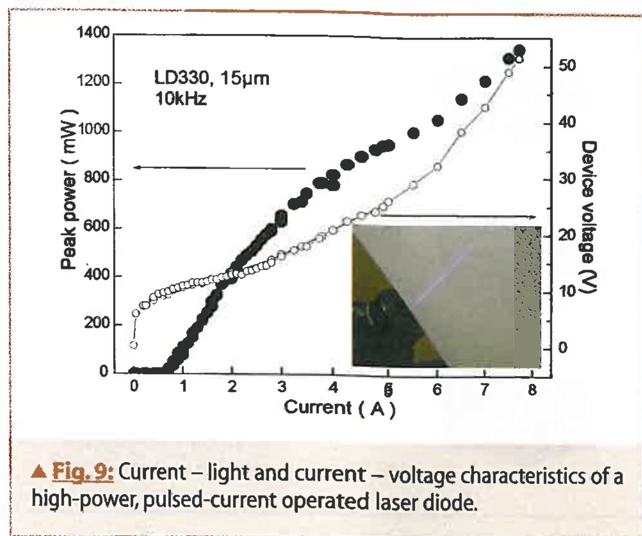

▲ Fig. 9: Current – light and current – voltage characteristics of a high-power, pulsed-current operated laser diode.

measured under pulsed current conditions (30 ns pulse length, 10 kHz repetition, room temperature). The maximum optical power per mirror was 1.3 W. Because of the symmetric coating, the total optical power can be stated to exceed 2.5 W, which makes this the largest optical power reported for nitride lasers [20].

The devices were life tested under constant current conditions and variable temperatures in the range of 35-70°C. The lifetime usually is defined as a time after which the optical power of the device (at constant current) decreases down to 50 % of its initial value. Accelerated tests predicts a lifetime approaching 10 000 h have been performed at the following conditions: current 1 A, frequency 100 kHz, pulse length 30 ns. The activation energy of the degradation processes was estimated to be 3.2 eV, similar to the value determined by Sony. No change in electrical properties of the devices was observed during aging. The mechanism of long-term degradation still remains undetermined.

Summary – present status and the future

Despite the big commercial success of blue and green LEDs based on (AlGaInN compound) compounds and an introduction blue and violet LDs to the market, the physical properties of GaN and InGaN and AlGaN systems are still not well understood. Similarly the technology of GaN devices is still far from maturity.

The main problem for technology based on freestanding HVPE grown GaN substrates is the reduction of the density of dislocations. The size of the substrates is already sufficient for many industrial application, however the dislocation densities still remain two orders of magnitude above the magic value 10^4 cm^{-2}, necessary for dislocation-free LDs that are especially important for high power LDs. The prospects for this method depend on whether the technology will be able to break this barrier in the near future.

The technology of blue lasers based on HNPSG single crystals has been able to provide dislocation-free laser structures, which has allowed record power to be obtained in the pulse mode operation. It has also brought the devices on the market—at present these devices are the only European devices on offer to customers.

The main areas, in which our blue laser technology should be improved, are:

- processing and heat management
- strain engineering
- p-type doping by magnesium.

But especially the move towards shorter wavelength (UV range) requires further progress in strain engineering to prevent

the generation of misfit dislocations and the cracking of AlGaN layers with higher aluminum content.

Acknowledgment

The research presented in this paper has been supported by Poland's Committee for Scientific Research grants 8 T11 G 001 2000 C/5013 and 7 T08A 015 18 and in part by the European Commission within the Support for Centers of Excellence No ICA1-CT-2000-70005 programme. The calculations were made using computing facilities of the Interdisciplinary Centre for Mathematical and Computational Modelling of Warsaw University.

References

[1] H. Amano, M. Kito, K. Hiramatsu, I. Akasaki. Jpn. J. Appl. Phys. Part 2-Letters, **28** (1989) L2112

[2] S. Nakamura, T. Mukai, M. Senoh, N. Iwasa, Jpn. J. Appl. Phys. Part 2-Letters .**31** (1992) L139

[3] J. M. Baranowski, in MRS Symposium Proceedings vol. 449, F. A. Ponce, T. D. Moustakas, I. Akasaki, B. A. Monemar, Editors, p. 393, Materials Research Society, Pittsburgh (1996)

[4] I. Grzegory, S. Krukowski, M. Leszczynski, P. Perlin, T. Suski, S. Porowski, Acta Phys. Pol. A Suppl. **100** (2001) 57

[5] Properties, Processing and Applications of Gallium Nitride and Related Semiconductors, ed. by J.H. Edgar, S.T. Strite, I. Akasaki, H. Amano and C. Wetzel, INSPEC-IEE London 1999

[6] S. Nakamura, M. Senoh, S. Nagahama, N. Iwasa, T. Yamada, T. Matsushita, H. Kiyoku, Y. Sugimoto, Jpn. J. Appl. Phys. **35** (1996) L217

[7] S.T. Kim, Y.J. Lee, D.C. Moon, C.H. Hong, T.K. Yoo J. Cryst. Growth **194** (1998) 37

[8] S. Nakamura IEICE Trans. **E83-C** (2000) 529-535

[9] J.L. Weyher, M. Albrecht, T. Wosinski, G. Nowak, H.P. Strunk, S. Porowski, Mater. Sci. Eng. **B80** (2001) 318

[10] W. Utsumi, H. Saitoh, H. Kaneko, T. Watanuki, K. Aoki, and O. Shimomura, Nature materials **2** (2003) 735

[11] I. Barin Thermochemical Data of Pure Substances 3rd edition, VCH Weinheim 1994

[12] E. Monberg, in Handbook of Crystal Growth 2. Bulk Crystal Growth A. Basic techniques ed by D.T.J. Hurle North-Holland Amsterdam 1994, p.51

[13] D.T.J. Hurle and B. Cockayne, in Handbook of Crystal Growth 2. Bulk Crystal Growth A. Basic techniques ed by D.T.J. Hurle North-Holland Amsterdam 1994, p.99

[14] J. Karpinski, J. Jun and S. Porowski, J. Cryst. Growth **66** (1984) 1

[15] Z. Romanowski. S. Krukowski, I. Grzegory, S. Porowski J. Chem. Phys. **114** (1990) 6353

[16] I. Grzegory, M. Boćkowski, B. Łucznik, S. Krukowski, Z.Romanowski, M. Wrtal Growth A. Basic techniques ed by D.T**246** (2002) 177

[17] M. Leszczynski, I. Grzegory, H. Teisseyre, T. Suski, M. Bockowski, J. Jun, J. M. Baranowski, S. Porowski and J. Domagala, J. Cryst. Growth **169** (1996) 235

[18] J. Domagala, M.Leszczynski, P. Prystawko, T. Suski, R. Langer, A Barski, M. Bremser J. Alloys Compounds **286** (1999) 284

[19] P. Prystawko, R. Czernecki, M. Leszczynski, P. Perlin, P. Wisniewski, L. Dmowski, H. Teisseyre, T. Suski, I. Grzegory, M. Bockowski, G. Nowak, S. Porowski, Phys. Status Solidi A **192** (2002) 320

[20] P. Perlin, M. Leszczyński, P. Prystawko, R. Czernetzki, P. Wisniewski, J.L. Weyher, G. Nowak, J. Borysiuk, L. Gorczyca, T, Swietlik, G. Franssen, A. Bering, C. Skierbiszewski, I. Grzegory , T. Suski and S. Porowski, Photonic West Conference Proceeding San Jose 2004

The stratosphere as a puppeteer of European winter climate

Peter Siegmund[1], Michael Sigmond[1,2], and Hennie Kelder[1,2]
[1]Royal Netherlands Meteorological Institute
[2]Technical University of Eindhoven

The depletion of the stratospheric ozone layer and the increase of greenhouse gas concentrations have led to changes in the climate of the stratosphere, the atmospheric layer between about 10 and 50 km. Stratospheric climate change currently receives wide attention among environmental physicists, because it will likely influence the speed of recovery of the ozone layer, and it may induce climate change in the troposphere, the atmospheric layer between the earth's surface and the stratosphere. Recent studies indicate that a significant part of the European winter warming observed in the past and predicted for the next decades might be due to changes in the climate of the stratosphere. To some extent the troposphere and the stratosphere might be regarded here as puppet and puppeteer, respectively. Unusually, the puppet's weight is about ten times that of the puppeteer.

Stratospheric ozone depletion

The ozone layer has been depleted due to human emissions of ozone-depleting gases containing chlorine and bromine. The ozone depletion is largest, about 50%, over Antarctica in winter-spring. This annually recurring "ozone hole" is due to special (photo)chemical ozone destruction reactions at very low temperatures that only occur in winter-spring over Antarctica and, to a lesser extent, the Arctic. Over the Arctic the depletion is up to about 20%, and is more variable than over Antarctica. Also at middle latitudes the ozone layer has been depleted, by about 5% between 1980 and 2000. As a result of international regulations, the total abundance of the ozone-depleting gases in the atmosphere has begun to decrease in recent years. Natural chemical and transport processes limit the rate at which these gases can be removed from the stratosphere. Model predictions indicate a recovery of the ozone layer to pre-ozone hole conditions by the middle of the 21st century. For more information about stratospheric ozone depletion see, e.g., Fahey *et al.* (2003).

Stratospheric global cooling

The ozone depletion leads to less absorption of solar radiation in the stratosphere and, consequently, to colder stratospheric temperatures. Also the increased greenhouse gas concentrations lead to colder stratospheric temperatures, which can be understood as follows. Greenhouse gases emit radiation at their local temperature, and absorb radiation that is emitted by the surrounding air, most of which is at lower altitudes. The emission increases with increasing temperature, according to Stefan-Boltzmann's law. Since in the stratosphere the temperature increases with altitude, the cooling by the emission at the local temperature exceeds the warming by the absorption of the radiation that is mainly emitted at the lower temperatures of the altitudes below. Thus in the stratosphere an increase in greenhouse gases will lead to more radiative cooling and,

features